

**Intracranial Volume and Head Circumference in Children with Unoperated Syndromic  
Craniosynostosis**

R. William F. Breakey MBBS BSc MRCS, Paul G.M. Knoops MSc, Alessandro Borghi MEng PhD, Naiara Rodriguez-Florez MEng PhD, Justine O'Hara FRCS(Plast), Gregory James PhD FRCS(Neuro. Surg.), David J. Dunaway FDSRCS FRCS(Plast), Silvia Schievano MEng PhD, N.U. Owase Jeelani MBA MPhil(Medical Law) FRCS(Neuro. Surg.)  
UCL GOS Institute of Child Health & Craniofacial Unit, Great Ormond Street Hospital for Children, NHS Trust, London, United Kingdom

**Corresponding Author:** William Breakey, UCL Great Ormond Street Institute of Child Health, 30 Guilford Street, WC1N 1EH, London, UK. +44 20 7242 9789,  
William.breakey@ucl.ac.uk

**Author Contributions:** RWFB, PGMK, GJ, NUOJ and SS designed the study, contributed to data acquisition, analysis and interpretation before drafting the manuscript. AB, NRF, JOH and DJD critically revised the manuscript.

**Acknowledgements:** This research was supported by Great Ormond Street Hospital Children's Charity FaceValue programme (no. 12SG15), The Royal College of Surgeons of England, and the EPSRC (EP/N02124X/1). This report incorporates independent research from the National Institute for Health Research Biomedical Research Centre Funding Scheme. The views expressed in this publication are those of the authors and not necessarily those of the NHS, the National Institute for Health Research or the Department of Health. None of the authors has a financial interest in any of the products, devices or drugs mentioned in this manuscript

This paper was presented at the 17<sup>th</sup> Congress of the International Society of Craniofacial Surgery on October 27<sup>th</sup> 2017 in Cancun, Mexico

ACCEPTED

## Abstract

**Objective:** When analysing intracranial volume gain due to operative intervention in craniosynostosis, it is necessary to understand the underlying growth. We sought to create comprehensive intracranial volume (ICV) and occipitofrontal circumference (OFC) growth charts, as measured on unoperated craniosynostotic children. Furthermore, we aimed to investigate whether ICV and OFC could act as a proxy measure for each other.

**Methods:** All pre-operative Great Ormond Street Hospital (GOSH) patients with a diagnosis of Apert, Crouzon-Pfeiffer or Saethre-Chotzen syndrome from 2004 onwards were considered for this study. A control group of unaffected GOSH patients were also measured. ICV and OFC were measured on the same scans. To study correlation between IVC and OFC, logarithmic fits were assessed.

**Results:** 147 craniosynostotic children with 221 preoperative scans were included (81 Apert, 81 Crouzon, 31 Pfeiffer, and 28 Saethre-Chotzen). The control group comprised 56 patients with 58 scans. Apert ICV curves were significantly larger than other syndromes from 206 days onwards, OFC curves were not significantly different. The correlation coefficient between ICV and OFC for all syndromes combined was  $R^2 = 0.87$ , for the control group  $R^2 = 0.91$ .

**Conclusions:** Apert children have a larger intracranial volume than other syndromic craniosynostotic conditions and unaffected children but maintain a similar occipitofrontal circumference. This study demonstrates high correlation between intracranial volume and OFC with clinical care implications. Reference growth curves have been created which can be used to monitor intracranial volume change over time and correct operative change for underlying growth.

## Introduction

Craniosynostosis describes a range of skull growth abnormalities. It can be either isolated, where one single suture is fused or present in multiple sutures. Isolated craniosynostosis is further defined by the suture that is fused, whilst multi-suture synostosis can be described as either ‘complex’ when no extracranial anomalies exist or ‘syndromic’ when associated with extracranial anomalies and frequently a known genetic cause.

The incidence of craniosynostosis as whole is estimated to be between 1 in 2,100 and 1 in 2,500 live births.<sup>1</sup> The premature unification of the cranial sutures can lead to multiple functional and aesthetic problems, with one of the earliest and most important being raised intracranial pressure (ICP)<sup>2</sup>, estimated to occur in 30-40% of all syndromic cases.<sup>3</sup> The exact cause of raised ICP in syndromic craniosynostosis is yet to be defined, once attributed to craniocerebral disproportion (in the absence of hydrocephalus)<sup>4</sup>, it is now thought more likely due to a combination of several factors including craniocerebral disproportion, venous hypertension<sup>5-7</sup>, hydrocephalus<sup>8</sup>, and airway obstruction<sup>9</sup>. This assumption was modified following a number of studies which showed that craniocerebral disproportion in craniosynostosis was likely only relevant for children < 1 year old, and that raised ICP can occur in the presence of a normal skull volume<sup>10,11</sup>

Intracranial volume (ICV) measurements, whilst not providing direct information about ICP, can provide information about the space available for the growing brain and give an indication as to whether craniocerebral disproportion may be present.<sup>10</sup> They can also be used to assess the change in volume gained by operative interventions;<sup>12</sup> however, as pre- and post-operative scans are often taken with significant time intervals, it may be necessary to take into account the underlying growth. Due to the current lack of syndrome specific growth curves, the underlying growth used in these cases is often taken from healthy children’s reference curves, which may not always be a true representation of syndromic growth.<sup>13</sup>

A variety of measurement techniques to determine ICV have been described in the literature, from early efforts relying on mathematical estimations<sup>14-16</sup> to more reliable, current practice methods based on 3-dimensional imaging from computed tomography (CT) or magnetic resonance (MR) scans. However, CT radiation exposure and the potential deleterious effects of a general anaesthetic required in a young child in MR, combined with lengthy image post-processing analysis, make regular surveillance of ICV in the same patient impractical. Rijken et al<sup>17</sup> (2015) illustrated the correlation between occipitofrontal circumference (OFC) and ICV; they suggested that OFC could be used as a marker of ICV, therefore overcoming the above problems. Whilst promising, the number of patients per syndrome in the study were small.

At Great Ormond Street Hospital for Children (GOSH), treatment for raised ICP is reactive rather than prophylactic. Thorough surveillance of ICP via ophthalmology including electrodiagnostic tests (visual evoked potentials) are included in the patient protocol.<sup>18</sup> Any deterioration, in concert with clinical evaluation indicating raised ICP would necessitate a vault expansion. Due to the reactive management of raised ICP at GOSH, we have a large cohort with a wide age range of unoperated children with syndromic craniosynostosis.

The aim of this work was twofold:

- 1) To provide syndrome specific reference growth curves to enable monitoring of ICV over time and allow for like-with-like comparison
- 2) To provide evidence for the use of OFC as an indicator of ICV

#### Methods

All pre-operative CT scans from GOSH patients with a diagnosis of Apert, Crouzon-Pfeiffer or Saethre-Chotzen syndrome were considered for this study. Crouzon and Pfeiffer patients were grouped together as one due to their shared FGFR2 mutations and the consideration that they can be phenotypic variations of the same genetic defect.<sup>19,20</sup> Scans were available from

2004 onwards. Exclusion criteria were: scans with slice thickness >3mm, incomplete scans that did not include the full region between the vertex and the foramen magnum, and scans that were obstructed by artefacts from shunt devices.

A cohort of non-craniofacial children was selected from the GOSH PACS database as control group. These patients underwent scanning in the period between January 2015 and January 2017. Other than those children with no known disease, diagnoses included haematological malignancies, epilepsy, extra cranial carcinomas, diabetic ketoacidosis and immune deficiencies. The CT scans were carried out to investigate: infection, haemorrhage, arterio-venous malformations, headaches, intracranial extension of dermoid cysts, cerebral oedema and craniosynostosis. None of the control patients had a history of head or craniofacial trauma. All control group scans were reports as normal by GOSH consultant radiologists, with no intracranial abnormalities. These scans were also required to be of a slice thickness <3mm and to include the vertex through to the foramen magnum.

ICV was calculated automatically using FSL (Analysis Group, FMRIB, Oxford, UK)<sup>21</sup>. In those cases where the automatic technique failed to extract the entire cranial vault, a semi-automatic approach using Simpleware ScanIP (Simpleware Ltd., Exeter, UK) was adopted. Simpleware requires the user to threshold each scan individually, before a region growing operation can produce a mask of the intracranial contents. Additional manual exclusion of areas outside the cranial vault is required before the program can calculate ICV using the voxel information within the mask. Both techniques have been shown to be reliable methods of ICV measurement, producing significantly similar results.<sup>22</sup>

OFC was performed on the same scan as the ICV measurement using CAD software Rhinoceros (McNeel Europe, & Associated, Seattle, WA, USA), which allows for a cutting plane to be visually selected at the perceived level of maximal head circumference. The head perimeter is then measured from the glabella to the occipital protuberance. This process is

undertaken three times to closely reflect the technique for measuring OFC in a clinical setting (Figure 1).

Correlation between IVC and OFC was studied in Matlab (Mathworks, Natick, MA, USA), with logarithmic fits accompanied by 95% confidence intervals as well as a coefficient of determination ( $R^2$ ) in all patient groups. The  $R^2$  is a statistical measure of how close data are to a fitted regression line. In general, the higher the  $R^2$  the better the model fits the data. The strength of the correlation can be described according to the guide produced by Evans<sup>23</sup> which suggests:

0.00-0.19: “very weak”

0.20-0.39: “weak”

0.40-0.59: “moderate”

0.60-0.79: “strong”

0.80-1.0: “very strong”

Normality of the data was assessed using the Shapiro-Wilk test. Two tailed Student t-test results were considered significant for  $p$  values  $<0.05$ . Statistical analyses were performed using SPSS.

## Results

There were 229 syndromic patients suitable for this study. Of these, 147 patients had 243 CT scans before any surgery was carried out. 221 of the pre-operative CT scans remained eligible for inclusion. This comprised 93 Apert scans (M:F 50:31), 117 Crouzon-Pfeiffer scans (M:F 67:45), and 33 Saethre-Chotzen (M:F 15:13) scans. The Pfeiffer children included in the study were either Type I or Type II / III, with 10/15 being type I. The older Pfeiffer children were all Type I (the oldest Type II / III child was 7 months old). The control group consisted of 56 patients with 58 eligible scans (M:F 33:25).

In the Apert cohort; 1 patient had a shunt in situ at the time of their scan, this was not excluded because the shunt had not caused any artefact and therefore did not affect the volume calculation, 6 patients went on to have a shunt after the scan used for ICV calculation. 18 patients have not required vault expansion for raised ICP, 35 patients have had posterior vault expansion at a time point following the scan used for ICV measurement. In the Crouzon-Pfeiffer cohort; 6 patients had shunts in situ at the time of their scan, 5 were not excluded because the shunt had not caused any artefact and therefore did not affect the volume calculation, 7 patients went on to have a shunt after the scan used for ICV calculation. Following the scan used for ICV measurement; 37 patients required cranial vault expansion, 15 required Monobloc and RED frame, 3 required Le Fort III, 1 patient underwent FOA and 15 have had no procedures to date.

In the Saethre-Chotzen cohort; no patients required shunting, 7 required cranial vault expansion, 8 required fronto-orbital advancement and 8 patients have yet to require a craniofacial procedure.

The mean age across all syndromic groups was 2.4 years (range 1 day to 17.5 years), whilst for the control group the mean age was 5.4 years (range 6 days to 15.7 years). For easier comparison, patients were further subdivided into 6 age ranges: 0 – 1y, 1 – 2y, 2 – 4y, 4 – 8y, 8 – 12y, 12 – 18y.<sup>17</sup> (Table 1).

Best fit logarithmic curves were assessed for ICV (Figure 2) and OFC (Figure 3) against time in all syndromes, and divided for gender (See Figure, Supplemental Digital Content 1, which shows the ICV growth curves for syndromic patients (black) and controls (blue), showing:

(A) male Apert patients and controls (B) female Apert patients and controls, (C) male Crouzon-Pfeiffer patients and controls and (D) female Crouzon-Pfeiffer patients and controls.

Solid line represents the fitted logarithmic curve, dashed lines represent 95% CI. The

equations provide the volume in  $\text{cm}^3$  when given age ( $x$ ) in days, INSERT HYPER LINK) (See Figure, Supplemental Digital Content 2, which shows the ICV growth curves for syndromic patients (black) and controls (blue), showing: (A) male Saethre-Chotzen patients and controls (B) female Saethre-Chotzen patients and controls. Solid line represents the fitted logarithmic curve, dashed lines represent 95% CI. The equations provide the volume in  $\text{cm}^3$  when given age ( $x$ ) in days, INSERT HYPER LINK) (See Figure, Supplemental Digital Content 3, which shows the OFC growth curves for syndromic patients (black) and controls (blue), showing: (A) male Apert patients and controls (B) female Apert patients and controls, (C) male Crouzon-Pfeiffer patients and controls and (D) female Crouzon-Pfeiffer patients and controls. Solid line represents the fitted logarithmic curve, dashed lines represent 95% CI. The equations provide the circumference in cm when given age ( $x$ ) in days, INSERT HYPER LINK) (See Figure, Supplemental Digital Content 4, which shows the OFC growth curves for syndromic patients (black) and controls (blue), showing: (A) male Saethre-Chotzen patients and controls (B) female Saethre-Chotzen patients and controls. Solid line represents the fitted logarithmic curve, dashed lines represent 95% CI. The equations provide the volume in  $\text{cm}^3$  when given age ( $x$ ) in days, INSERT HYPER LINK). For ICV, mean  $R^2$  for the syndromic groups was 0.75, for the control group  $R^2$  was 0.80. For OFC, mean  $R^2$  for the syndromic groups was 0.76 and control group  $R^2$  was 0.86. Average head growth was overall similar for all syndromes and the control groups, apart from Apert patients. Apert ICV began to diverge from the control group at 63 days, becoming significantly different at day 206. (Figure 4). ICV and OFC were highly correlated for all syndromes ( $R^2 = 0.87$ , male  $R^2 = 0.85$ , female  $R^2 = 0.87$ ) and for the control group ( $R^2 = 0.91$ , male  $R^2 = 0.88$ , female  $R^2 = 0.93$ ). ICV against OFC correlations for control, Apert, Crouzon-Pfeiffer and Saethre-Chotzen patients are shown in Figure 5. These have been further subdivided into sex specific correlations in the supplementary figures (See Figure, Supplemental Digital Content 5, which shows the ICV

against OFC growth curves for syndromic patients (black) and controls (blue), showing: (A) male Apert patients and controls (B) female Apert patients and controls, (C) male Crouzon-Pfeiffer patients and controls and (D) female Crouzon-Pfeiffer patients and controls. Solid line represents the fitted logarithmic curve, dashed lines represent 95% CI. The equations provide the volume in  $\text{cm}^3$  when given circumference ( $x$ ) in cm, [INSERT HYPER LINK](#) (See Figure, Supplemental Digital Content 6, which shows the ICV against OFC growth curves for syndromic patients (black) and controls (blue), showing: (A) male Saethre-Chotzen patients and controls (B) female Saethre-Chotzen patients and controls. Solid line represents the fitted logarithmic curve, dashed lines represent 95% CI. The equations provide the volume in  $\text{cm}^3$  when given age ( $x$ ) in days, [INSERT HYPER LINK](#)). Figure 4 provides an overview of ICV, OFC, and ICV vs OFC for all subjects. Figure 4A shows the marked difference in Apert ICV as compared to the other groups, whereas Figure 4B shows overall similarity in OFC.

Mean ICV and OFC across all groups and subdivided age ranges are shown in Table 2. There was no significant ICV differences between Crouzon-Pfeiffer and control, or Saethre-Chotzen and control at any age group, nor with Apert and control in the 0-1y age group. From the 1-2y age group and upwards, there was a significant difference throughout (1-2 y  $p=0.03$ , 2-4 y  $p=0.01$ , 4-8 y  $p=0.02$ , 8-12 y  $p<0.01$ , 12-18 y  $p<0.01$ )

## Discussion

In literature, there is a lack of specific reference curves for ICV in patients with syndromic craniosynostosis. Having access to craniofacial growth curves offers the clinician an opportunity to directly compare clinical findings to published normal data. In the clinic, one can quickly assess whether a patient's growth curve is deflecting from the norm (an OFC not changing or showing growth of  $<0.5$  SD within 2 years is a risk factor for developing papilloedema)<sup>17</sup>, and therefore have a higher level of suspicion for raised intracranial

pressure. When planning vault expansion surgery, the surgical team can use normal data to estimate a required percentage increase in intracranial volume. Post-operatively, by correcting for the underlying growth, change in volume can be assessed. In this study, we have produced reference curves in a large series of children with Apert, Crouzon-Pfeiffer and Saethre-Chotzen syndromes and provided the necessary equations to transform OFC data into ICV estimates.

Apert children have a larger ICV when compared to the control group, in keeping with previous studies<sup>24,25</sup>. The Apert group shows a similar ICV growth trajectory to the control group initially. After day 206, Apert ICV is significantly larger when the 95% CI no longer overlap (Figure 2A). This divergence agrees with the significant difference between Apert ICV and Control ICV seen from the 1-2 year age group and onwards. This was not found in the Crouzon-Pfeiffer and Saethre-Chotzen groups, which is illustrated clearly by Figure 4. ICV is highly correlated with OFC in Apert, and, when compared to the control group, the line of best fit is shifted superiorly, indicating a larger ICV for a given OFC, in line with the phenotypical turricephalic head shape often seen in Apert children. Male Apert children have a larger ICV than female Apert children, suggesting that sex specific growth curves should be used when referencing.

The Crouzon-Pfeiffer cohort ICV showed increased spread throughout the study timeframe (Figure 2B). This was reflected in the  $R^2$  being the lowest of all groups. ICV against OFC in this group remained strongly correlated. There were fewer Saethre-Chotzen patients available for this study, leaving a cohort of 15 males and 13 females, but the trends were still clear, also with strong correlation for ICV against OFC.

In each syndrome cohort there were a number of outliers. We believe that this can be explained in part by the phenotypic variation seen in craniofacial syndromes, especially in Crouzon-Pfeiffer<sup>26</sup>. A further factor to consider in the Crouzon-Pfeiffer group is the Cohen

classification of the Pfeiffer children who were either Type I or Type II / III, with 10/15 being type I. The older Pfeiffer children were all Type I (the oldest Type II / III child was 7 months old). This is likely to have contributed to the spread of results in the Crouzon-Pfeiffer. There are visible outlying data points in the Apert cohort. These can be seen lying superiorly to the line of best fit.

Raised ICP has been extensively reported in children with syndromic craniosynostosis with Tamburrini et al documenting a 30-40% prevalence.<sup>3</sup> Difficulty remains however in determining what is a normal childhood ICP, and this has led to a wide range of incidences reported in the literature.<sup>10</sup> Thompson et al. showed a 65% incidence of raised ICP in Crouzon Syndrome, 60% in Pfeiffer, 43% in Saethre-Chotzen and 38% in Apert Syndrome<sup>27</sup>, whereas Marucci et al. found the incidence of raised ICP in Apert syndrome to be 83%<sup>28</sup>. Both studies measured ICP transcranially and used mean pressures of greater than 15mmHg over 24 hours to indicate raised ICP.

In a further study, Renier and colleagues studied ICV and ICP in craniosynostosis, and noted that volume measurement does not give a reliable indication of ICP, however in the presence of raised ICP, there will also be restricted skull growth.<sup>2</sup> Interestingly, children with Apert syndrome who have been confirmed in this study as having larger ICV are still at risk of raised ICP. There appears to be little difference in ICV between the Crouzon-Pfeiffer, Saethre-Chotzen and control groups, indeed no group had a significantly lower ICV than the control which differs from the establishment of craniosynostosis preventing skull and potentially brain growth. This would add further weight to the argument that raised ICP is not entirely caused by craniocerebral disproportion.<sup>10,24,29</sup>

The strong correlation between ICV and OFC provides a useful proxy in the clinical setting or if the time-consuming measurement of ICV was not available. The OFC is easily obtained in clinic and reproducible, and where as it has previously been described as a crude

technique,<sup>30</sup> reflecting skull base growth rather than volume, we have found it to closely relate to ICV across our control group and all syndromic groups. Especially interesting was the strength of the correlation in Apert syndrome, where despite the turricephaly an  $R^2$  of 0.9 was observed.

It should be noted that our control group is taken from a cohort of Great Ormond Street Hospital for Children patients, with normal head scans. Whilst the study benefits from both the syndromic patients and the control group being measured via the same technique, this may have introduced a bias in the control group. However, comparison of our control data with a study on the ICV in healthy children up to 72 months of age by Kamdar et al<sup>31</sup> has shown similar behaviour, we found our 95% confidence interval to overlap with their growth curve, thus implying our control group matches a normal control group.

Normative growth curves are at their most accurate when very large populations have been included in the data collection. As with all single centre studies on rare syndromes, our work is limited by low subject numbers. This is especially evident when further breaking down our data by syndrome and sex. We must acknowledge a limitation to the study here as there is potential for our data to be skewed by these low numbers.

## Conclusion

In this study, we have provided reference intracranial volume and occipitofrontal circumference growth curves for unoperated children with syndromic craniosynostosis, as well as a control group. This could allow craniofacial clinicians and researchers to adjust for underlying growth when calculating a change in volume to be attributed to a surgical procedure, and serve as a rapid tool to estimate intracranial volume from occipitofrontal circumference measurements. In our cohort we have shown that Apert children have larger ICVs than control children after the age of 6.7 months, whilst Crouzon-Pfeiffer and Saethre-Chotzen ICVs remain similar to controls and that no group had significantly different OFCs.

## References

1. Johnson D, Wilkie AOM. Craniosynostosis. *Eur J Hum Genet.* 2011;19(4):369-376. doi:10.1038/ejhg.2010.235.
2. Gault DT, Renier D, Marchac D, Jones BM. Intracranial pressure and intracranial volume in children with craniosynostosis. *Plast Reconstr Surg.* 1992;90(3):377-381. doi:10.1097/00006534-199209000-00003.
3. Tamburrini G, Caldarelli M, Massimi L, Santini P, Di Rocco C. Intracranial pressure monitoring in children with single suture and complex craniosynostosis: A review. *Child's Nerv Syst.* 2005;21(10):913-921. doi:10.1007/s00381-004-1117-x.
4. Dominique Renier, M.D., Christian Sainte-Rose, M.D., Daniel Marchac, M.D., and Jean-Francois Hirsch MD. Intracranial pressure changes in craniostenosis. *J.* 1982;57(9):370-377. doi:10.3171/jns.1982.57.3.0370.
5. Hayward R. Venous hypertension and craniosynostosis. *Child's Nerv Syst.* 2005;21(10):880-888. doi:10.1007/s00381-004-1114-0.
6. Taylor WJ, Hayward RD, Lasjaunias P, et al. Enigma of raised intracranial pressure in patients with complex craniosynostosis: the role of abnormal intracranial venous drainage. *J Neurosurg.* 2001;94(3):377-385. doi:10.3171/jns.2001.94.3.0377.
7. Rich PM, Cox TCS, Hayward RD. The jugular foramen in complex and syndromic craniosynostosis and its relationship to raised intracranial pressure. *Am J Neuroradiol.* 2003;24(1):45-51.
8. Collmann H, Sörensen N, Krauß J. Hydrocephalus in craniosynostosis: A review. *Child's Nerv Syst.* 2005;21(10):902-912. doi:10.1007/s00381-004-1116-y.
9. Gonzalez S, Hayward R, Jones B, Lane R. Upper airway obstruction and raised intracranial pressure in children with craniosynostosis. *Eur Respir J.* 1997;10(2):367-

375. doi:10.1183/09031936.97.10020367.
10. Fok H, Jones BM, Gault DG, Andar U, Hayward R. Relationship between intracranial pressure and intracranial volume in craniosynostosis. *Br J Plast Surg*. 1992;45(5):394-397. doi:10.1016/0007-1226(92)90013-N.
  11. Sgouros S. Skull vault growth in craniosynostosis. *Child's Nerv Syst*. 2005;21(10):861-870. doi:10.1007/s00381-004-1112-2.
  12. Serlo WS, Ylikontiola LP, Lähdesluoma N, et al. Posterior cranial vault distraction osteogenesis in craniosynostosis: Estimated increases in intracranial volume. *Child's Nerv Syst*. 2011;27:627-633. doi:10.1007/s00381-010-1353-1.
  13. Derderian CA, Wink JD, McGrath JL, Collinsworth A, Bartlett SP, Taylor JA. Volumetric Changes in Cranial Vault Expansion. *Plast Reconstr Surg*. 2015;135(6):1665-1672. doi:10.1097/PRS.0000000000001294.
  14. Sgouros S, Goldin JH, Hockley a D, Wake MJ, Natarajan K. Intracranial volume change in childhood. *J Neurosurg*. 1999;91:610-616. doi:10.3171/jns.1999.91.4.0610.
  15. Bray PF, Shields DW, Wolcott GJ, Madsen JA. Occipitofrontal bead measure of intracranial. *J Pediatr*. 1969;75(2):303-305.
  16. Tng TTH, Chan TCK, Hagg U, Cooke MS. Validity of cephalometric landmarks . An experimental study on human skulls. *Eur J Orthod*. 1994;16:110-120.
  17. Rijken BFM, den Ottelander BK, van Veelen M-LC, Lequin MH, Mathijssen IMJ. The occipitofrontal circumference: reliable prediction of the intracranial volume in children with syndromic and complex craniosynostosis. *Neurosurg Focus*. 2015;38(5: E9):1-6.
  18. Liasis A, Thompson DA, Hayward R, Nischal KK. Sustained raised intracranial pressure implicated only by pattern reversal visual evoked potentials after cranial vault expansion surgery. *Pediatr Neurosurg*. 2003;39(2):75-80. doi:10.1159/000071318.
  19. Cunningham ML, Seto ML, Ratisoontorn C, Heike CL, Hing A V. Syndromic

- craniosynostosis: From history to hydrogen bonds. *Orthod Craniofacial Res.* 2007;10(2):67-81. doi:10.1111/j.1601-6343.2007.00389.x.
20. Spruijt B, Rijken BFM, den Ottelander BK, et al. First vault expansion in Apert and Crouzon-Pfeiffer syndromes: Front or Back. *Plast Reconstr Surg.* 2015;1. doi:10.1097/PRS.0000000000001894.
21. Muschelli J, Ullman NL, Mould WA, Vespa P, Hanley DF, Crainiceanu CM. Validated automatic brain extraction of head CT images. *Neuroimage.* 2015;114:379-385. doi:10.1016/j.neuroimage.2015.03.074.
22. Breakey W, Knoops PGM, Borghi A, et al. Intracranial Volume Measurement: A Systematic Review and Comparison of Different Techniques. *J Craniofac Surg.* 2017;28(7). doi:10.1097/SCS.00000000000003929.
23. Evans JD. *Straightforward Statistics for the Behavioural Sciences.* Pacific Grove, CA: Brooks/Cole Publishing. Pacific Grove, CA: Brooks/Cole Publishing; 1996.
24. Anderson PJ, Netherway DJ, Abbott AH, Cox T, Roscioli T, David DJ. Analysis of intracranial volume in Apert syndrome genotypes. *Pediatr Neurosurg.* 2004;40(4):161-164. doi:10.1159/000081933.
25. Gosain a K, McCarthy JG, Glatt P, Staffenberg D, Hoffmann RG. A study of intracranial volume in Apert syndrome. *Plast Reconstr Surg.* 1995;95(2):284-295. doi:10.1097/00006534-199502000-00008.
26. Carinci F, Pezzetti F, Locci P, et al. Apert and Crouzon Syndromes: Clinical Findings, Genes and Extracellular Matrix. *J Craniofac Surg.* 2005;16(3):361-368. doi:10.1097/01.SCS.0000157078.53871.11.
27. Thompson DN., Jones BM, Harkness WJ, Gonsalez S, Hayward RD. Consequences of Cranial Vault Expansion Surgery for Craniosynostosis. *Pediatr Neurosurg.* 1997;26:296-303.

28. Marucci DD, Dunaway DJ, Jones BM, Hayward RD. Raised intracranial pressure in Apert syndrome. *Plast Reconstr Surg*. 2008;122(4):1162-1168-1170.  
doi:10.1097/PRS.0b013e31818458f0.
29. Abu-Sittah GS, Jeelani O, Dunaway D, Hayward R. Raised intracranial pressure in Crouzon Syndrome: incidence, causes and management. *J Neurosurg Pediatr*. 2016;17(9):469-475. doi:DOI: 10.3171/2015.6.PEDS15177.
30. Sgouros S, Hockley a D, Goldin JH, Wake MJ, Natarajan K. Intracranial volume change in craniosynostosis. *J Neurosurg*. 1999;91:617-625.  
doi:10.3171/jns.1999.91.4.0617.
31. Kamdar MR, Gomez RA, Ascherman J a. Intracranial volumes in a large series of healthy children. *Plast Reconstr Surg*. 2009;124(6):2072-2075.  
doi:10.1097/PRS.0b013e3181bcefc4.

## Figure Legends

Figure 1 – OFC measured using Rhinoceros with a technique that closely matches clinical measurement.

Figure 2. ICV growth curves showing: (A) Apert patients, (B) Crouzon-Pfeiffer patients, (C) Saethre-Chotzen patients, (D) Control patients. Solid line represents the fitted logarithmic curve, dashed lines represent 95% CI. The equations provide the volume in  $\text{cm}^3$  when given age ( $x$ ) in days.

Figure 3. OFC growth curves showing: (A) Apert patients, (B) Crouzon-Pfeiffer patients, (C) Saethre-Chotzen patients, (D) Control patients. Solid line represents the fitted logarithmic curve, dashed lines represent 95% CI. The equations provide the circumference in cm when given age ( $x$ ) in days.

Figure 4. Summary graphs for all subjects showing: (A) ICV against time, (B) OFC against time, and (C) ICV vs OFC correlation

Figure 5. ICV against OFC correlations for: (A) Apert patients, (B) Crouzon-Pfeiffer patients, (C) Saethre-Chotzen patients and (D) Control patients. The equations provide the volume in  $\text{cm}^3$  when given circumference ( $x$ ) in cm.

Supplemental Digital Content 1. See Figure, which shows the ICV growth curves for syndromic patients (black) and controls (blue), showing: (A) male Apert patients and controls (B) female Apert patients and controls, (C) male Crouzon-Pfeiffer patients and controls and (D) female Crouzon-Pfeiffer patients and controls. Solid line represents the fitted logarithmic curve, dashed lines represent 95% CI. The equations provide the volume in  $\text{cm}^3$  when given age ( $x$ ) in days, [INSERT HYPER LINK](#).

Supplemental Digital Content 2. See Figure, which shows the ICV growth curves for syndromic patients (black) and controls (blue), showing: (A) male Saethre-Chotzen patients and controls (B) female Saethre-Chotzen patients and controls. Solid line represents the fitted

logarithmic curve, dashed lines represent 95% CI. The equations provide the volume in  $\text{cm}^3$  when given age ( $x$ ) in days, [INSERT HYPER LINK](#).

Supplemental Digital Content 3. See Figure, which shows the OFC growth curves for syndromic patients (black) and controls (blue), showing: (A) male Apert patients and controls (B) female Apert patients and controls, (C) male Crouzon-Pfeiffer patients and controls and (D) female Crouzon-Pfeiffer patients and controls. Solid line represents the fitted logarithmic curve, dashed lines represent 95% CI. The equations provide the circumference in cm when given age ( $x$ ) in days, [INSERT HYPER LINK](#).

Supplemental Digital Content 4. See Figure, which shows the OFC growth curves for syndromic patients (black) and controls (blue), showing: (A) male Saethre-Chotzen patients and controls (B) female Saethre-Chotzen patients and controls. Solid line represents the fitted logarithmic curve, dashed lines represent 95% CI. The equations provide the volume in  $\text{cm}^3$  when given age ( $x$ ) in days, [INSERT HYPER LINK](#).

Supplemental Digital Content 5. See Figure, which shows the ICV against OFC growth curves for syndromic patients (black) and controls (blue), showing: (A) male Apert patients and controls (B) female Apert patients and controls, (C) male Crouzon-Pfeiffer patients and controls and (D) female Crouzon-Pfeiffer patients and controls. Solid line represents the fitted logarithmic curve, dashed lines represent 95% CI. The equations provide the volume in  $\text{cm}^3$  when given circumference ( $x$ ) in cm, [INSERT HYPER LINK](#).

Supplemental Digital Content 6. See Figure, which shows the ICV against OFC growth curves for syndromic patients (black) and controls (blue), showing: (A) male Saethre-Chotzen patients and controls (B) female Saethre-Chotzen patients and controls. Solid line represents the fitted logarithmic curve, dashed lines represent 95% CI. The equations provide the volume in  $\text{cm}^3$  when given age ( $x$ ) in days, [INSERT HYPER LINK](#).

Table Legend

Table 1. Age group demographics across all syndromes

Table 2. Mean ICV and OFC across all age groups and syndromes

ACCEPTED

Age	Crouzon-				Syndrome totals
	Apert	Pfeiffer	Saethre-Chotzen	Control	
zero – one	44	52	12	12	108
one – two	10	21	8	9	39
two - four	11	17	4	9	32
four - eight	7	11	3	8	21
eight- twelve	4	5	0	13	9
twelve - eighteen	5	6	1	7	12
Mean Age (years)	2.6	2.45	2.1	5.4	
Minimum Age (years)	0.0	0.0	0.2	0	
Maximum Age (years)	17.2	17.5	12.7	15.7	

Table 1. Age group demographics across all syndromes

Age	Apert		Crouzon-Pfeiffer		Saethre-Chotzen		Control	
	ICV(cm <sup>3</sup> )	OFC(cm)	ICV (cm <sup>3</sup> )	OFC (cm)	ICV(cm <sup>3</sup> )	OFC(cm)	ICV(cm <sup>3</sup> )	OFC (cm)
zero - one	792.5	39.8	829.6	41.5	835.8	41.3	831.8	42.7
one - two	1363.9	46.8	1208.7	47.5	1097.8	46.4	1115.4	47.6
two - four	1450.6	49.4	1332.3	48.7	1281.9	48.3	1189.7	48.8
four - eight	1625.8	50.3	1459.2	50.7	1309.0	50.7	1364.1	51.2
eight- twelve	1691.5	52.0	1328.6	50.3			1439.1	53.4
twelve - 18	1760.8	55.3	1360.6	53.2	1361.1	55.4	1318.0	53.1

Table 2. Mean ICV and OFC across all age groups and syndromes.

ACCEPTED

**Figure 1**



Figure 2

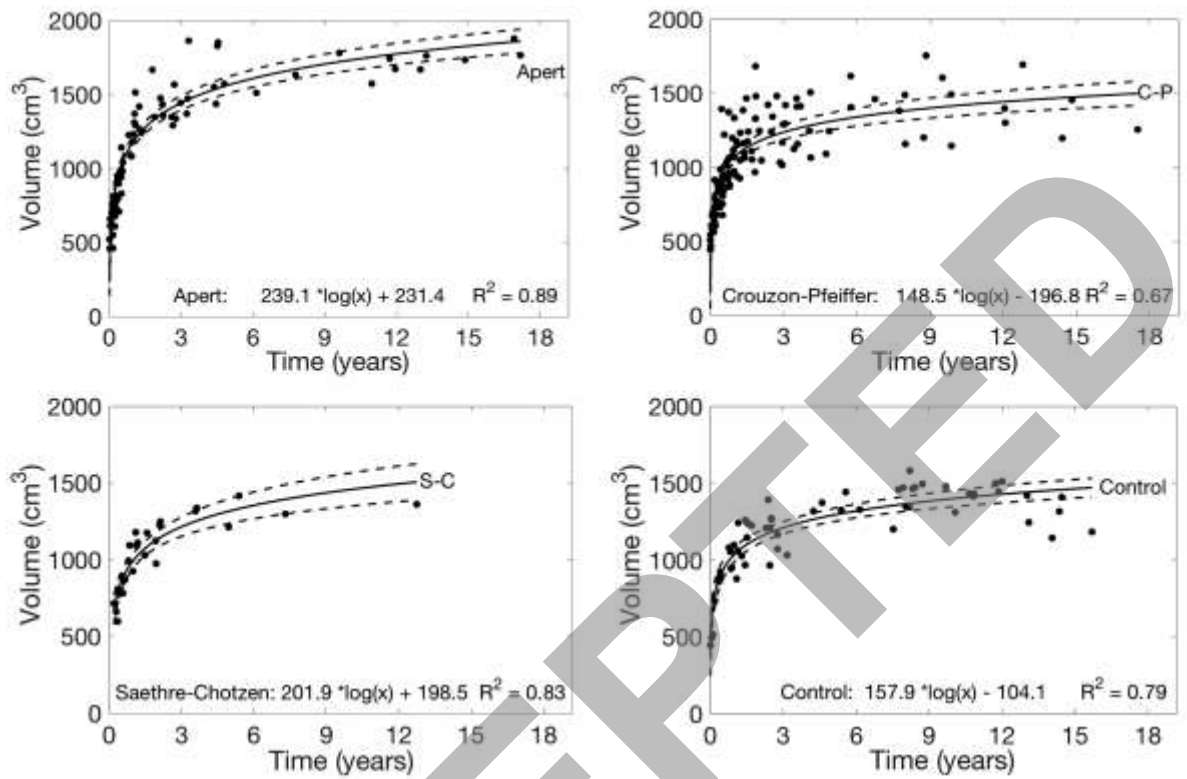


Figure 3

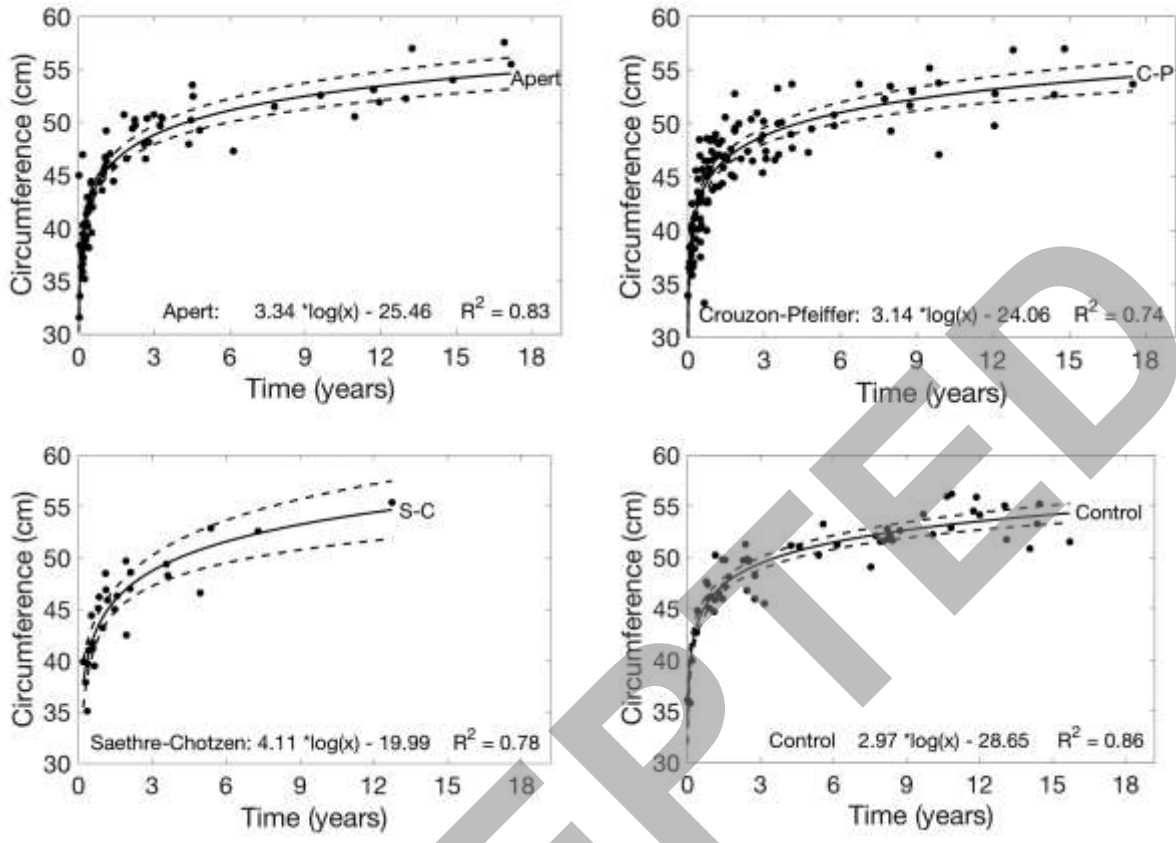


Figure 4

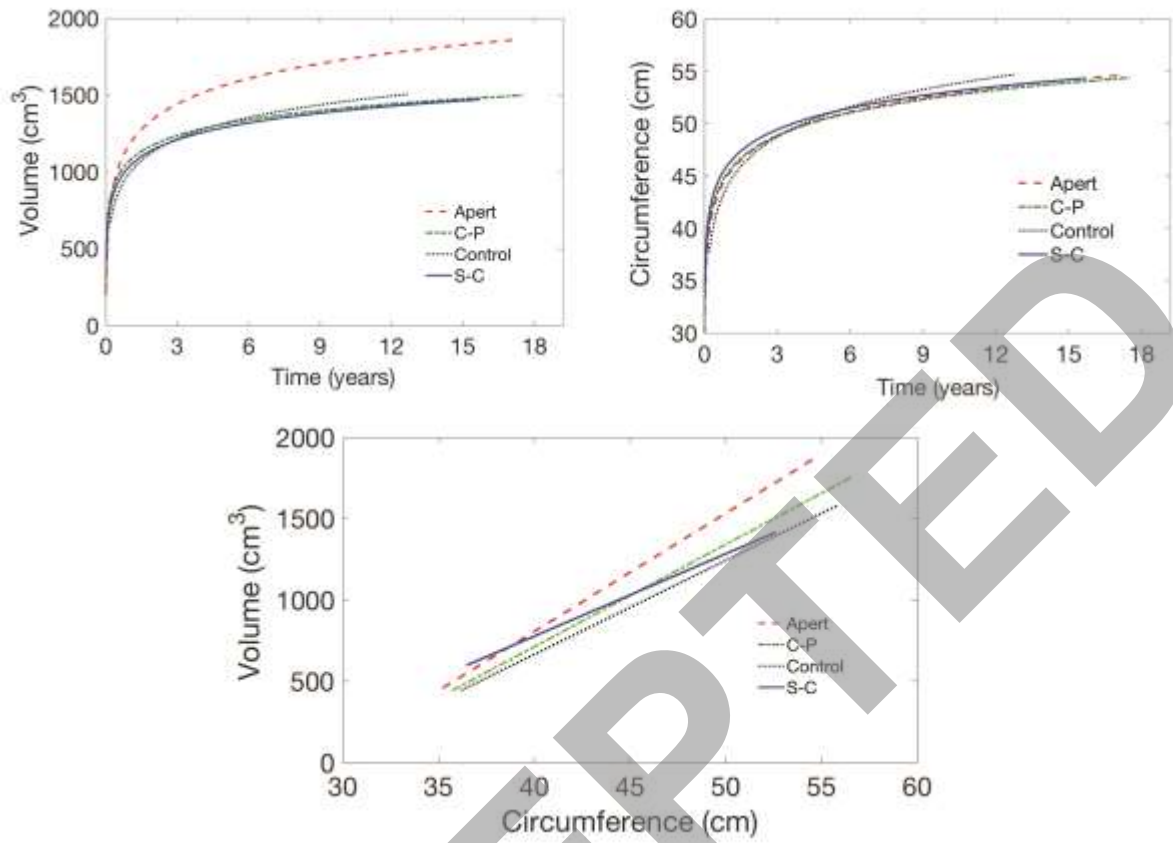
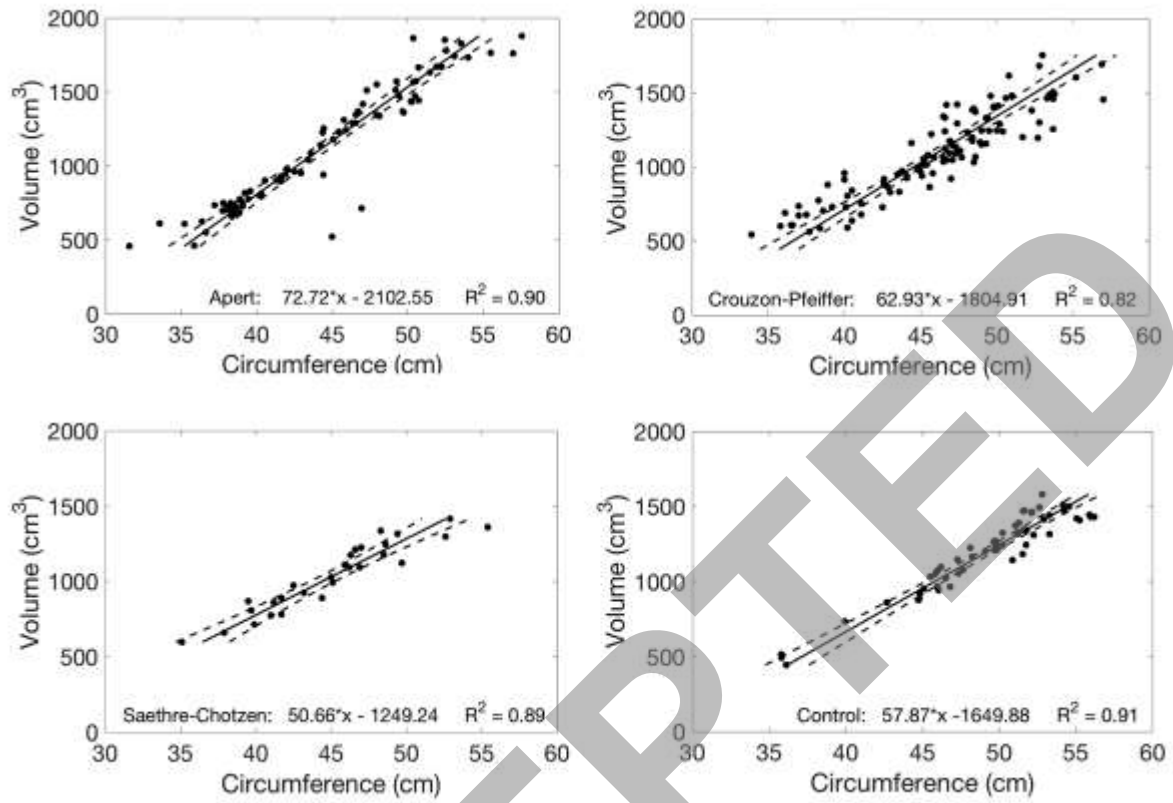
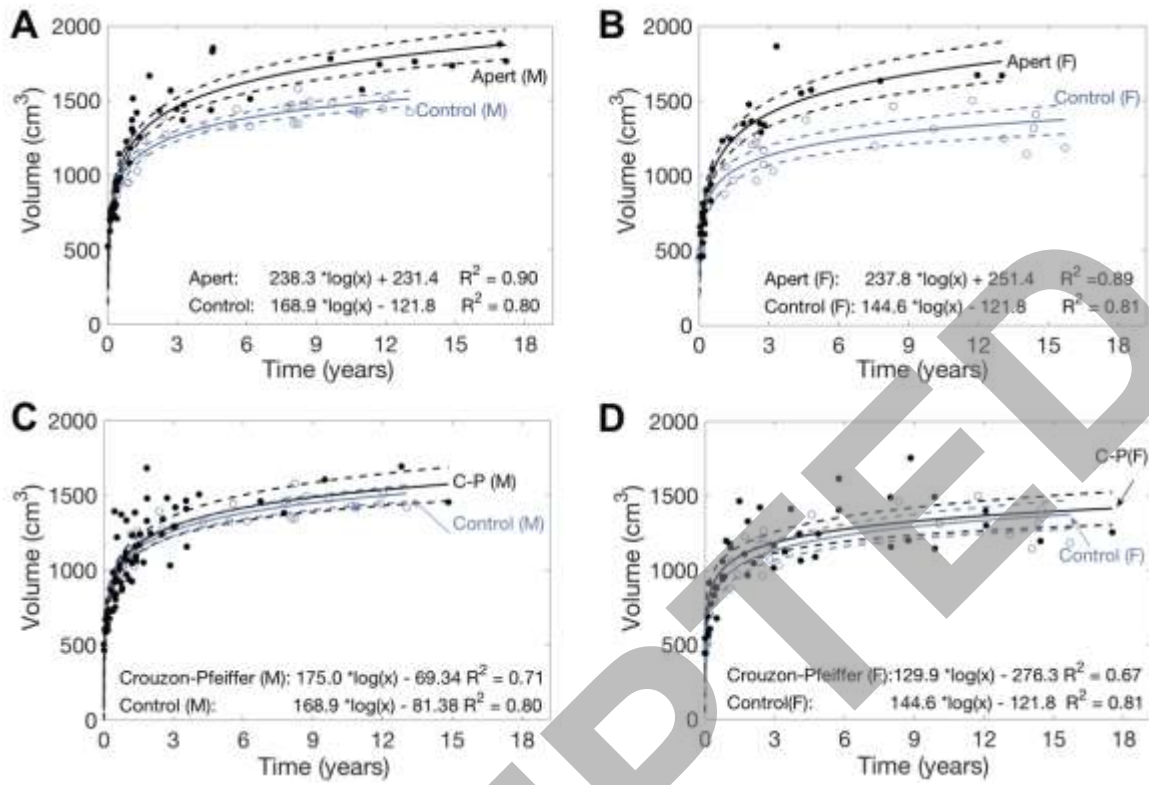


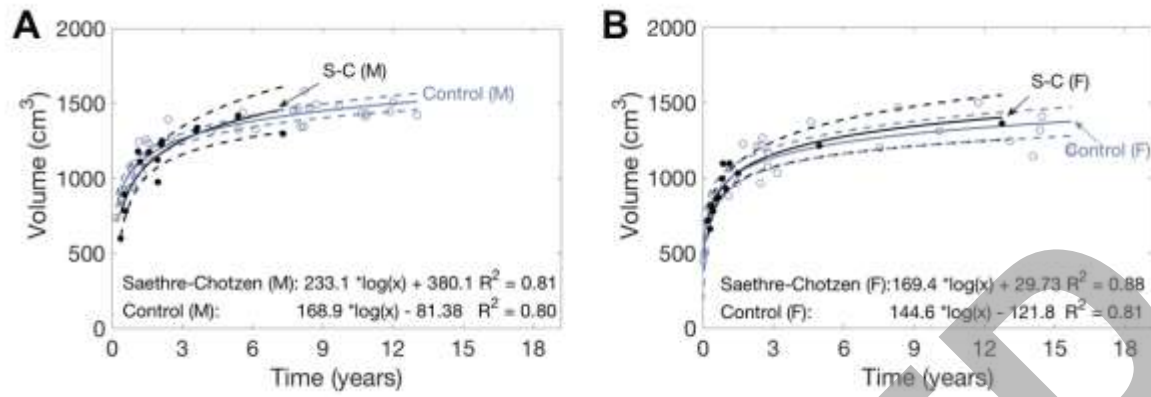
Figure 5



SDC 1

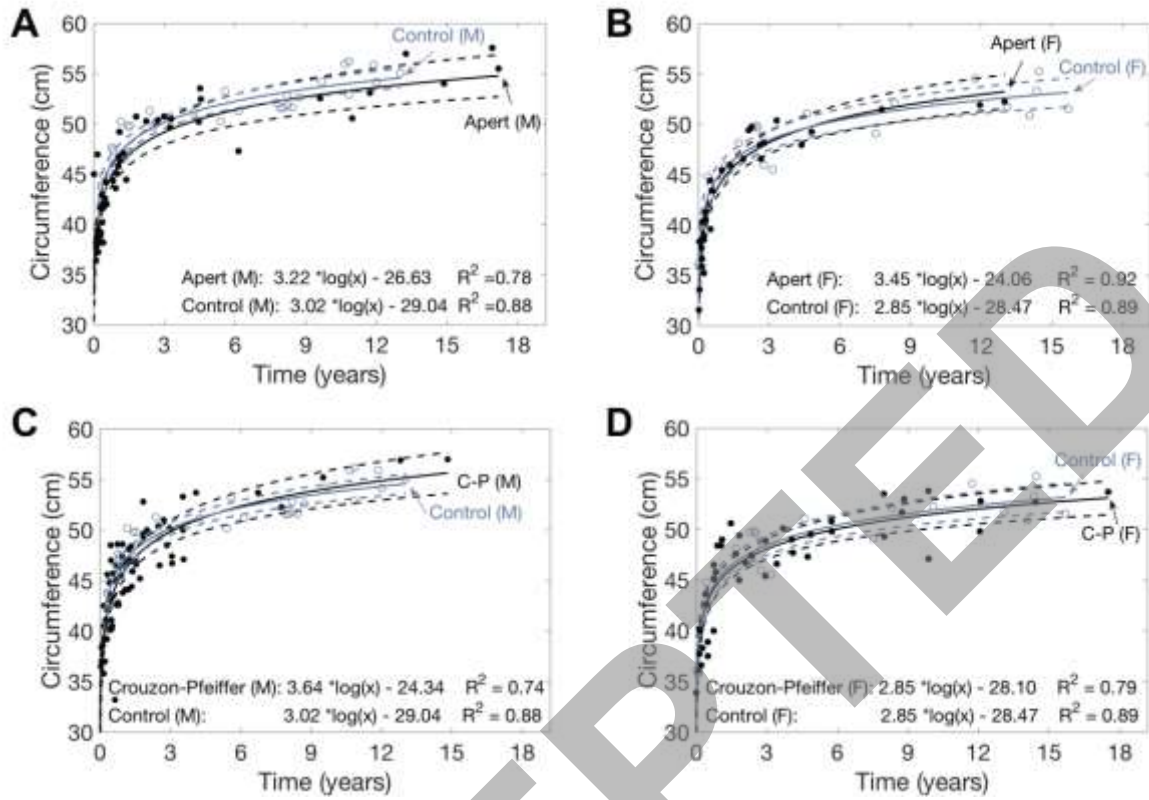


SDC 2

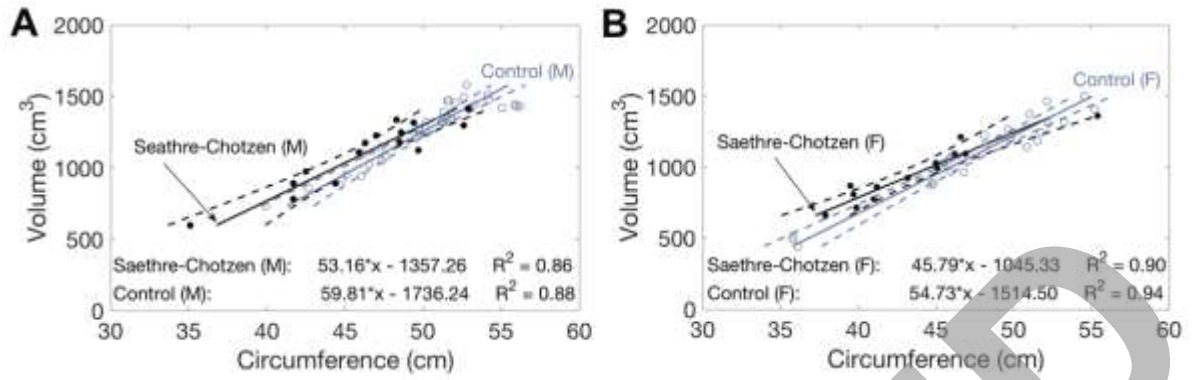


ACCEPTED

SDC 3

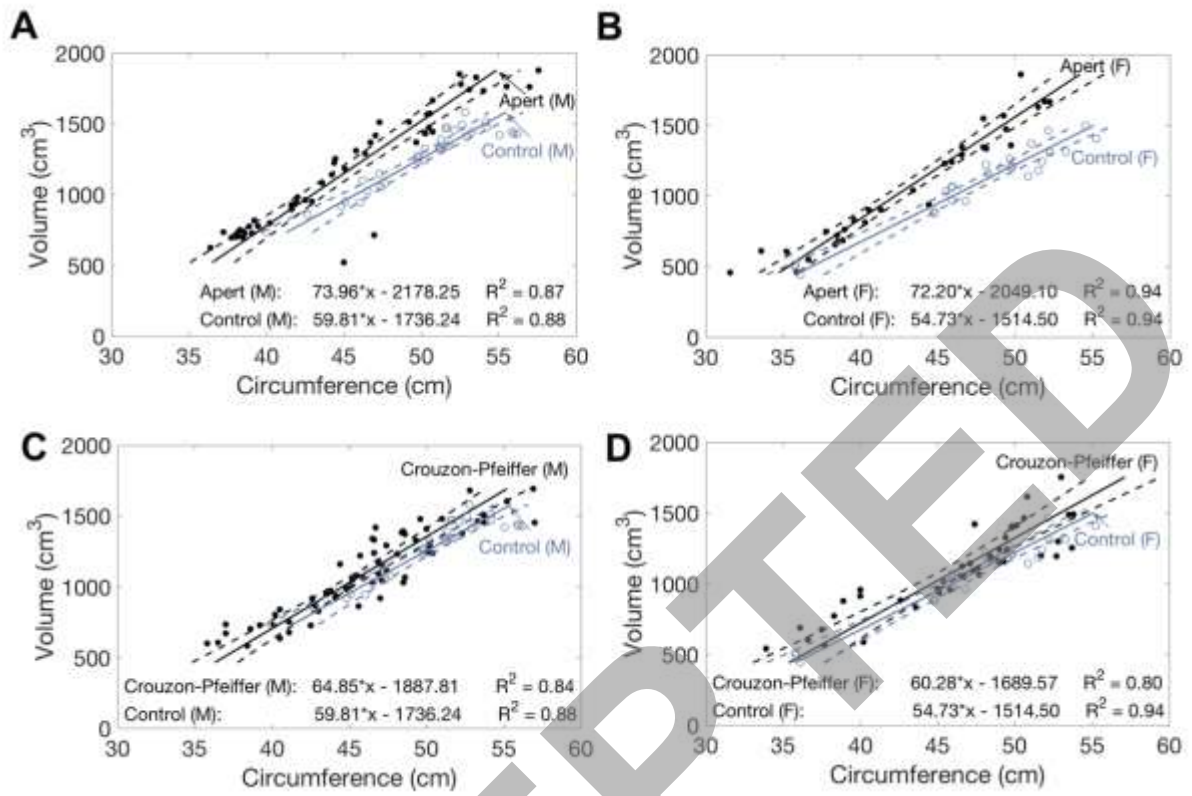


SDC 4



ACCEPTED

SDC 5



SDC 6

